

Supporting Information

Yu et al. 10.1073/pnas.0905165106

SI Experimental Procedures

Materials. Peptides were synthesized in a 96-well format using a MultiPep from Intavis Bioanalytical Instruments AG. Preloaded NovaSyn Tentagel resins and fluorenylmethoxycarbonyl-derivatized phosphoamino acid monomers were from Novabiochem. Heavy-isotope phosphopeptides were synthesized at 2- μ mol scale and contained one residue of L-Pro-N-Fmoc (U-13C5, 97–99%; 15N, 97–99%) (CNLM-4347, Cambridge Isotope Laboratories). Normal-isotope peptides were made at 5- μ mol scale. Amino acids activated in situ with 1-H-benzotriazolium, 1-[bis(dimethylamino)methylene]-hexafluorophosphate (1-),3-oxide:1-hydroxybenzotriazole hydrate and 4-methylmorpholine were coupled at a 5-fold molar excess over peptide. Each coupling cycle was followed by capping with acetic anhydride to avoid accumulation of 1-residue deletion peptide byproducts. After synthesis, peptide-resins were treated with a standard scavenger-containing trifluoroacetic acid-water cleavage solution, and the peptides were precipitated by addition to cold ether. Peptides were purified by semipreparative HPLC separation and quantified with 2,4,6-trinitrobenzenesulphonic acid (1).

Antibodies against the following proteins were used for Western blot analysis: phospho-RSK (Thr-359/Ser-363), RSK, Akt, phospho-Akt (Ser-473), ERK1/2, phospho-S6 (Ser-235/236), phospho-PI3K regulatory subunit p85(Tyr-467)/p55(Tyr-199), actin, histone H3, Src, phospho-Src (Tyr-416), EGFR, phosphotyrosine(*p*-Tyr-100), phospho-threonine-proline (*p*-Thr-Pro-101) (Cell Signaling Technology), phospho-ERK1/2 (Thr-202/Tyr-204) (Sigma), PI3 kinase regulatory subunit p55 γ (Santa Cruz Biotechnology), pan-PI3 kinase regulatory subunit p85 (Millipore), and PI3 kinase catalytic subunit p110 α (BD Biosciences). UO126 and wortmannin were obtained from Sigma and SU6656 was purchased from Calbiochem. Recombinant Akt1, RSK1, Src, and EGFR were purchased from Cell Signaling Technology.

Cell Culture, Transfection, and Lysis. HEK293 cells were maintained in Dulbecco's modified Eagle's medium (DMEM) supplemented with 10% FBS (FBS). For cell lysis, the media were removed, and cells were washed with ice-cold PBS and lysed with ice-cold LB lysis buffer (10 mM K₂HPO₄ pH 7.5, 1 mM EDTA, 10 mM MgCl₂, 50 mM β -glycerophosphate, 5 mM EGTA, 0.5% Nonidet P-40, 0.1% Brij 35, 0.1% deoxycholic acid, 1 mM sodium orthovanadate, 1 mM phenylmethyl-sulfonyl fluoride, 5 μ g/ml leupeptin and 5 μ g/ml pepstatin A). Lysates were centrifuged at 10,000 \times *g* for 10 min to remove cell debris, and clear supernatant was used for immunoblot and in vitro kinase assays. Protein concentration was determined by Bradford assay (Bio-Rad).

After a 16-h starvation period, HEK293 cells were treated with insulin (100 nM, 10 min), EGF (50 ng/ml, 5 min), or PMA (50 ng/ml, 10 min) at 37 °C for the indicated times. For drug inhibition studies, cells were pretreated with UO126 (5 μ M) or wortmannin (100 nM) for 30 min before mitogen stimulation. For the small interfering RNA (siRNA) studies, 21 nucleotide complementary RNA with symmetrical 2 nucleotide overhangs were obtained from Qiagen. The DNA sequences against which double-stranded RNAs for RSK1 and RSK2 were created were CCCAACATCATCACTCTGAAA and AGCGCTGAGAATGGACAGCAA, respectively. HEK293 cells were transfected using the calcium-phosphate procedure using 1 to 2 μ g each siRNA per 100-mm dishes. Transfection efficiency was determined to be greater than 95% using a fluorescently labeled mock

siRNA. Twenty-four hours following transfection, cells were serum-starved for 16 to 18 h, stimulated with EGF, and then harvested. The lysates were centrifuged for 10 min at 4 °C, and immunoblotted as shown.

For preparation of cell lysates in cell-cycle experiments, thymidine stock solution was added to HeLa cells at final concentration of 2.5 mM for 19 h. Cells were then washed with 25 ml PBS 3 times and released in growth media for 9 h. Then, thymidine stock was applied to the cells again for another 16-h culture. After double thymidine block, half of the G1/S cells were harvested and stored for later use, the other half was washed with PBS 3 times and immediately released into nocodazole containing light media at a final concentration of 0.2 μ g/ml until 90% of cells were rounded up. G2/M cells were collected by mitotic shake-off.

Cell Culture of Breast Cancer Cell Lines. MCF7 and MBA-MB231 cells were maintained in DMEM supplemented with 10% FBS. Sum159 cells were maintained in Ham's F12 media supplemented with 5% FBS, 5- μ g/ml insulin and 1- μ g/ml hydrocortisone. MCF10A, MCF10A/ErbB2, MCF10A/IGFR, and MCF10A/H-Ras^{G12V} cells were generously provided by J. Brugge (2–4) and were maintained in 50/50 DMEM/F12 media supplemented with 5% horse serum, 20 ng/ml EGF, 100 ng/ml cholera toxin, 10 μ g/ml insulin, and 500 ng/ml hydrocortisone. Breast cancer cells were also treated with 1 μ M of gefitinib (LC laboratories) for 24 h before lysis and KAYAK analysis. The mutation data (Fig. 6A) was obtained from the Wellcome Trust Sanger Institute Cancer Genome Project Web site, <http://www.sanger.ac.uk/genetics/CGP> and ref. 5.

Western Blot. Lysates were resolved on 4 to 12% SDS/PAGE, transferred onto Protran membranes (Whatman), blocked with 3% milk in TBST, incubated with a 1:1,000 dilution of primary antibody at 4 °C overnight, washed, and incubated with a 1:5,000 dilution of secondary antibody (HRP-conjugated) in 3% milk in TBST for 1 h at room temperature. Bands were visualized with ECL solutions (6).

Sample Preparation, MS Analysis, and Kinase Activity Quantitation. All reactions were performed using 6- μ g cell lysate (unless otherwise noted). Each lysate aliquot was mixed to a final volume of 20 μ l containing 25 mM Tris pH 7.5, 5 mM ATP, 100 μ M peptide substrate, 7.5 mM MgCl₂, 0.15 mM EGTA, 7.5 mM β -glycerol phosphate, 0.1 mM sodium orthovanadate, 0.1 mM DTT. The reaction was incubated at 25 °C for 60 min and then terminated by the addition of 100 μ l of 1% trifluoroacetic acid containing a known amount of ISTD (typically 20 pmol). Forty-five individual in vitro kinase reaction mixtures were combined and desalted by using Sep-Pak C18 cartridges (Waters). Phosphopeptides were enriched by immobilized metal ion chromatography with 20 μ l of beads (Phos-Select iron affinity gel, Sigma) and subsequently desalted by using Empore C18 solid phase extraction disks (3M) as described previously (7).

Samples were analyzed with an LTQ-FT or LTQ-orbitrap mass spectrometer (ThermoFisher) using LC-MS conditions described previously (7). Briefly, peptides were separated on a hand-pulled fused silica microcapillary (125 μ M \times 15 cm, packed with Magic C18AQ, Michrom Bioresources) using a 45-min linear gradient ranging from 10% to 37% acetonitrile in 0.1% formic acid. For each cycle, one full, high-resolution MS scan was acquired (10⁶ ion AGC setting), followed by two

MS/MS scans in the linear ion trap. MS/MS experiments were performed for phosphorylation site localization.

Quantification of the target peptide-internal standard ratios was performed by first constructing the extracted ion chromatogram for the most abundant charge state for each peptide using a ± 10 -ppm window around the monoisotopic peak. Chromatograms were integrated using Qual/Quan browser (Xcalibur 2.0.5,

Thermo Fisher). Because the phosphorylated peptides generated from the in vitro kinase reactions were chemically identical to the internal standards, they were assumed to have the same ionization efficiency. Therefore, the amount of each phosphorylated peptide was calculated by direct ratio to the internal standard level.

1. Fields R (1971) The measurement of amino groups in proteins and peptides. *Biochem J* 124:581–590.
2. Debnath J, et al. (2002) The role of apoptosis in creating and maintaining luminal space within normal and oncogene-expressing mammary acini. *Cell* 111:29–40.
3. Irie HY, et al. (2005) Distinct roles of Akt1 and Akt2 in regulating cell migration and epithelial-mesenchymal transition. *J Cell Biol* 171:1023–1034.
4. Reginato MJ, et al. (2003) Integrins and EGFR coordinately regulate the pro-apoptotic protein Bim to prevent anoikis. *Nat Cell Biol* 5:733–740.
5. Hollestelle A, et al. (2007) Phosphatidylinositol-3-OH kinase or RAS pathway mutations in human breast cancer cell lines. *Mol Cancer Res* 5:195–201.
6. Roux PP, et al. (2004) Tumor-promoting phorbol esters and activated Ras inactivate the tuberous sclerosis tumor suppressor complex via p90 ribosomal S6 kinase. *Proc Natl Acad Sci USA* 101:13489–13494.
7. Villen J, Beausoleil SA, Gerber SA, Gygi SP (2007) Large-scale phosphorylation analysis of mouse liver. *Proc Natl Acad Sci USA* 104:1488–1493.
8. Beausoleil SA, et al. (2006) A probability-based approach for high-throughput protein phosphorylation analysis and site localization. *Nat Biotechnol* 24:1285–1292.
9. Huang CH, et al. (2007) The structure of a human p110alpha/p85alpha complex elucidates the effects of oncogenic PI3Kalpha mutations. *Science* 318:1744–1748.

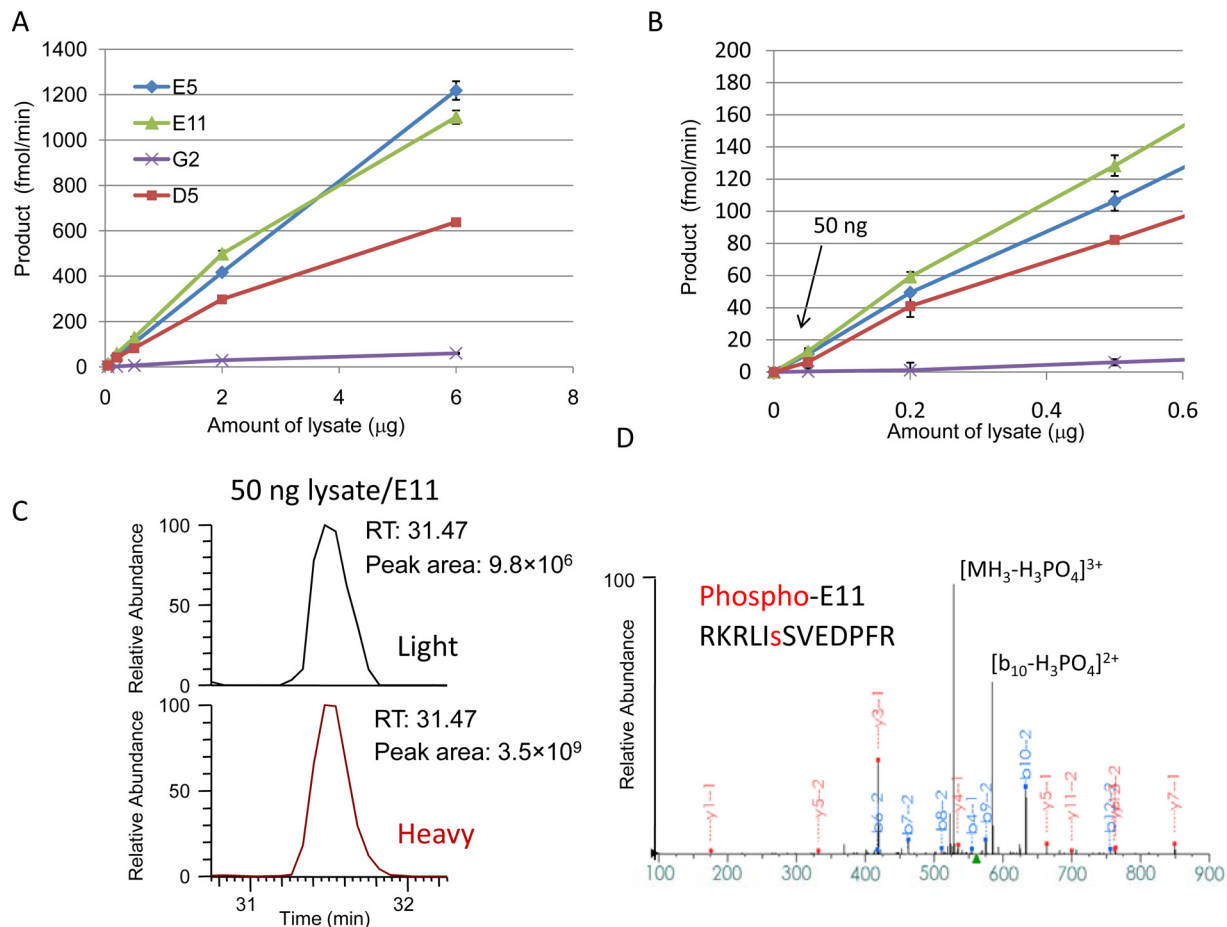


Fig. S1. Linearity and sensitivity of the KAYAK method. (A) Activities toward several representative peptides were measured using from 50-ng to 6- μg lysate of insulin-stimulated HEK293 cells. The KAYAK assay was performed using varying amount of cell lysate but constant substrate concentration (100 μM) and reaction time (1 h). Substrate peptide responses were linear across all lysate levels. (B) Expanded view of the low-end region. (C) One representative extracted ion chromatogram of the light and heavy phospho-E11 peptide using 50 ng of the lysate. A ± 10 -ppm mass tolerance around the monoisotopic peak was used. Retention time (RT) and area under the curve are shown. No signal was detected for the light peptide at the zero time point. The amount of phosphorylated peptide formed was calculated to be 770 fmol, which is still 100 times above the limit of quantification for nanoscale chromatography coupled to high-resolution MS (≈ 1 fmol). (D) MS/MS spectrum of the light phosphorylated E11 peptide. Sequence was determined to be RKRLI_sSVEDPFR.

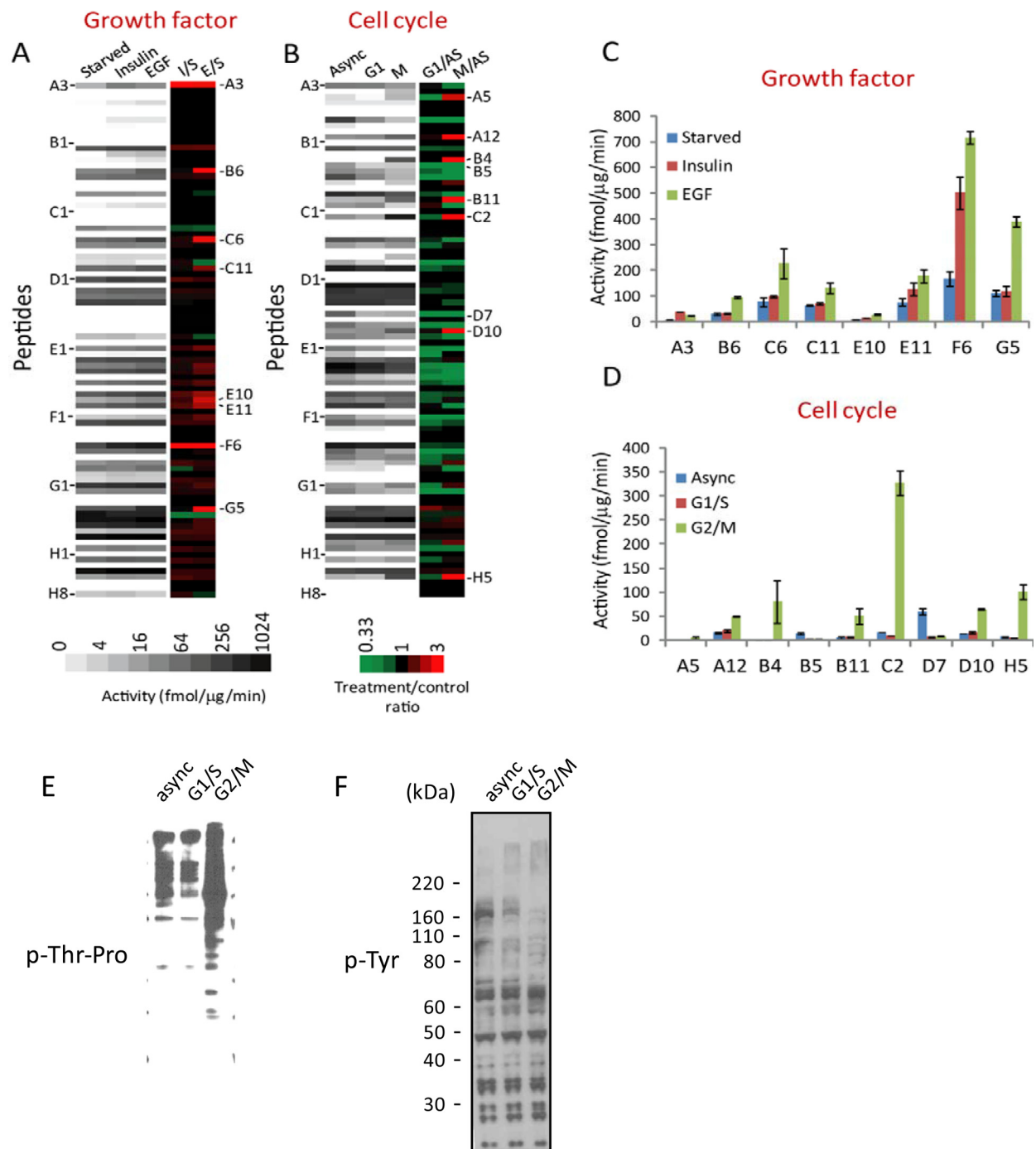


Fig. S2. Peptide phosphorylation rates accurately report pathway activation states. (A) Intensity map of kinase activities of starved (S), insulin-stimulated (I) and EGF-stimulated (E) HEK293 cells (average of triplicate experiments). Fold change over the starved state is also shown. Peptides with signals below detection threshold were not included for ratio calculation. (B) Intensity map of kinase activities of asynchronously growing (AS) HeLa cells, and cells arrested in either G1/S or G2/M phase of the cell cycle. Fold change over the asynchronous state is also shown. Peptides were ordered according to their positions in the 96-well plate. (C) Peptides with altered phosphorylation rates after insulin or EGF stimulation from 3 separate experiments. (D) Peptides with altered phosphorylation activities during cell cycle. Sequences of all peptides can be found in [Table S1](#). (E) Immunoblotting analysis of lysates of asynchronously growing HeLa cells and cells arrested in G1/S and G2/M phase using a general antiphospho-threonine-proline motif antibody. Proline-directed phosphorylation increased in G2/M. (F) Immunoblot analysis of lysates of asynchronously growing HeLa cells and cells arrested in G1/S and G2/M phase using a general anti-phospho-tyrosine antibody.

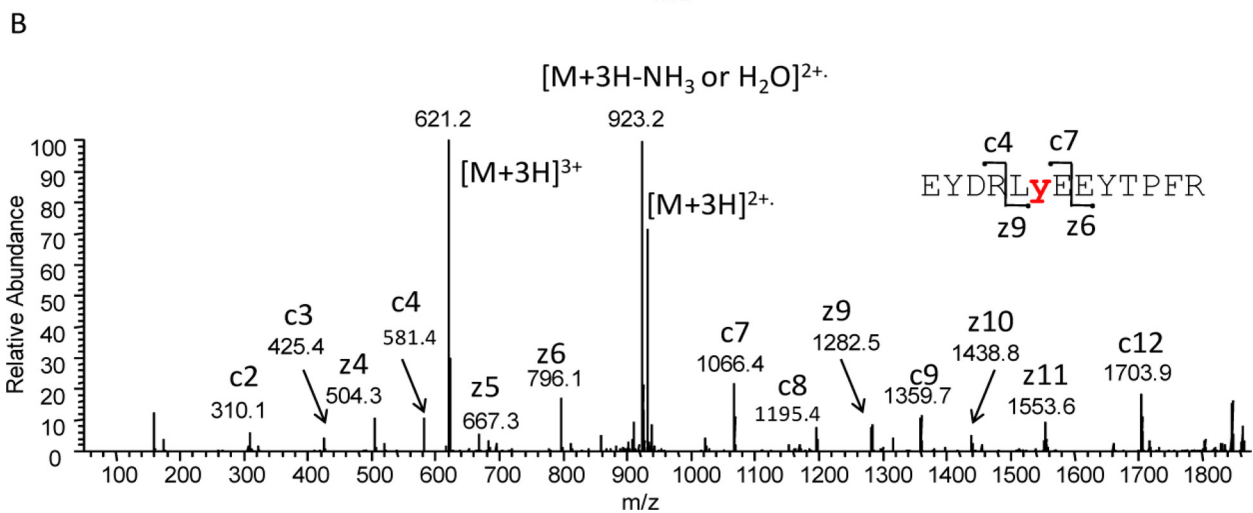
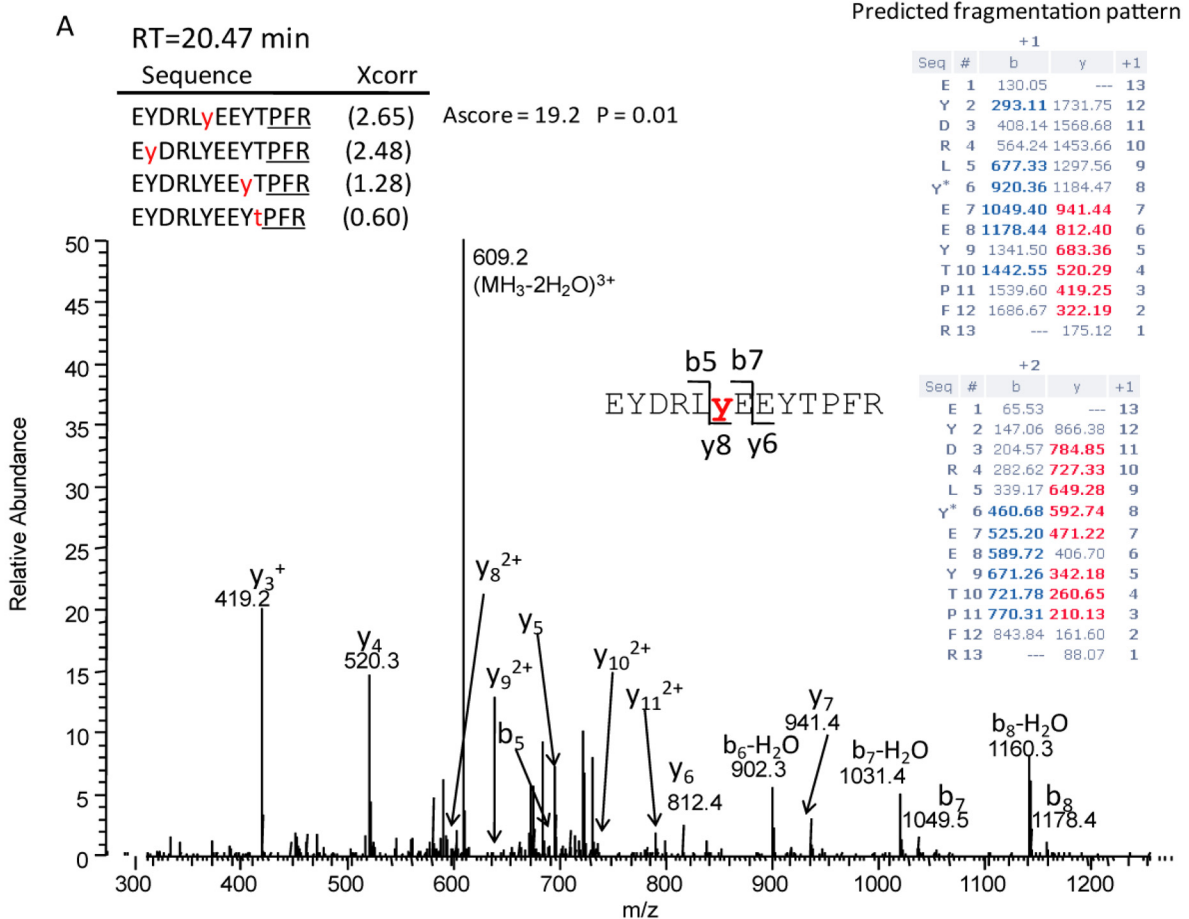


Fig. S3. Phosphate localization of the H5 peptide. (A) H5 peptide was phosphorylated using nocodazole arrested HeLa cell lysate and phospho-H5 was subjected to collision-induced dissociation MS/MS analysis. The correct phosphorylation site was localized with an Ascore (8) of 19.2 ($P = 0.01$). (B) electron transfer dissociation MS/MS spectrum of the phospho-H5 peptide. Site-determining ions for the designated sequence (EYDRLyEEYTPFR) are shown.

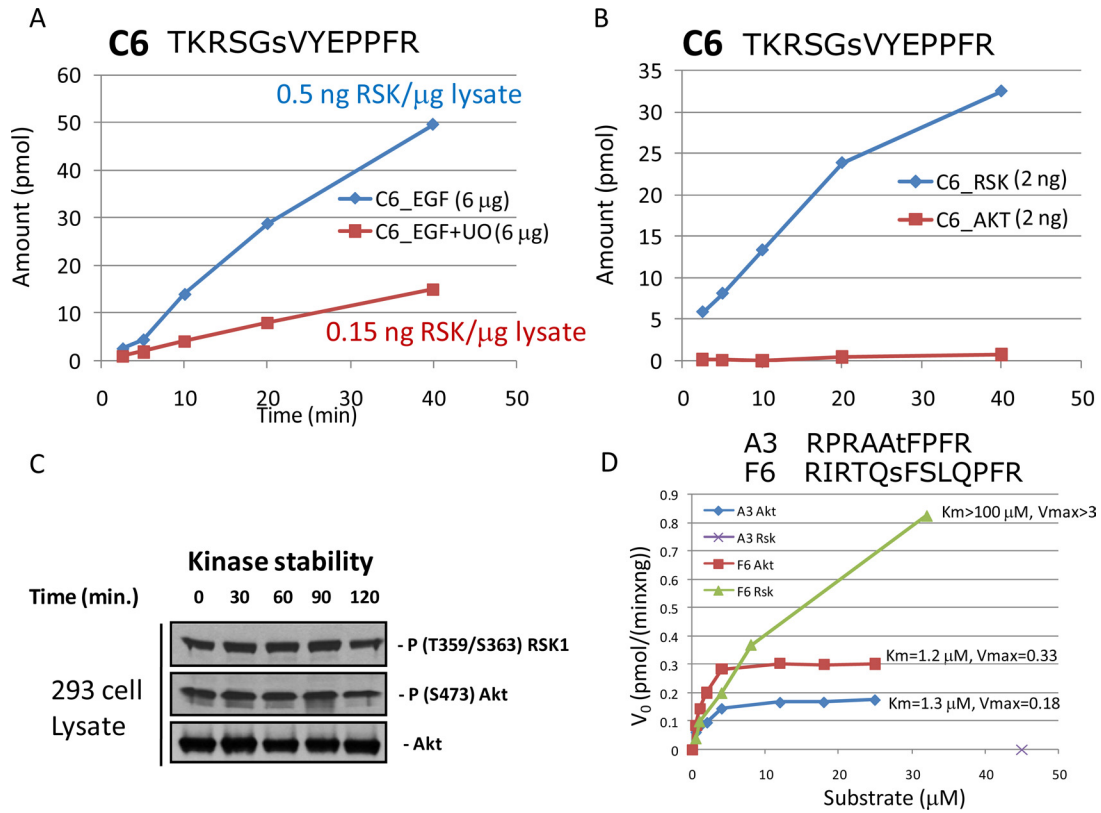


Fig. S5. Phosphorylation of peptides by cell lysates and purified kinases. (A) C6 was phosphorylated by EGF-stimulated HEK293 cell lysates and the lysates of HEK293 cells pretreated with UO126 and then stimulated with EGF. Reaction conditions were the same as those indicated in *Experimental Procedures*. From the data, we estimated the amount of active RSK present in these lysates. (B) C6 was phosphorylated in vitro using 2 ng of activated, purified Akt1 and RSK1. Reaction mixture was supplemented with 0.1% BSA. Other conditions were the same as in (A). (C) Western blot analysis of the lysates used in these KAYAK experiments. Kinase levels and phosphorylation states were stable in these reaction conditions. (D) Kinase specificity can be tuned by decreasing the reaction substrate concentration. F6 peptide is derived from a reported Akt site within nitric oxide synthase. We found that both Akt and RSK1 can phosphorylate this peptide using purified enzymes. The kinetics, however, were very different. RSK phosphorylation is preferred at concentrations $>10 \mu\text{M}$ and Akt phosphorylation is preferred at $<5 \mu\text{M}$. A3 peptide is provided for comparison and is not phosphorylated by RSK1 (RSK1 is a serine-only kinase).

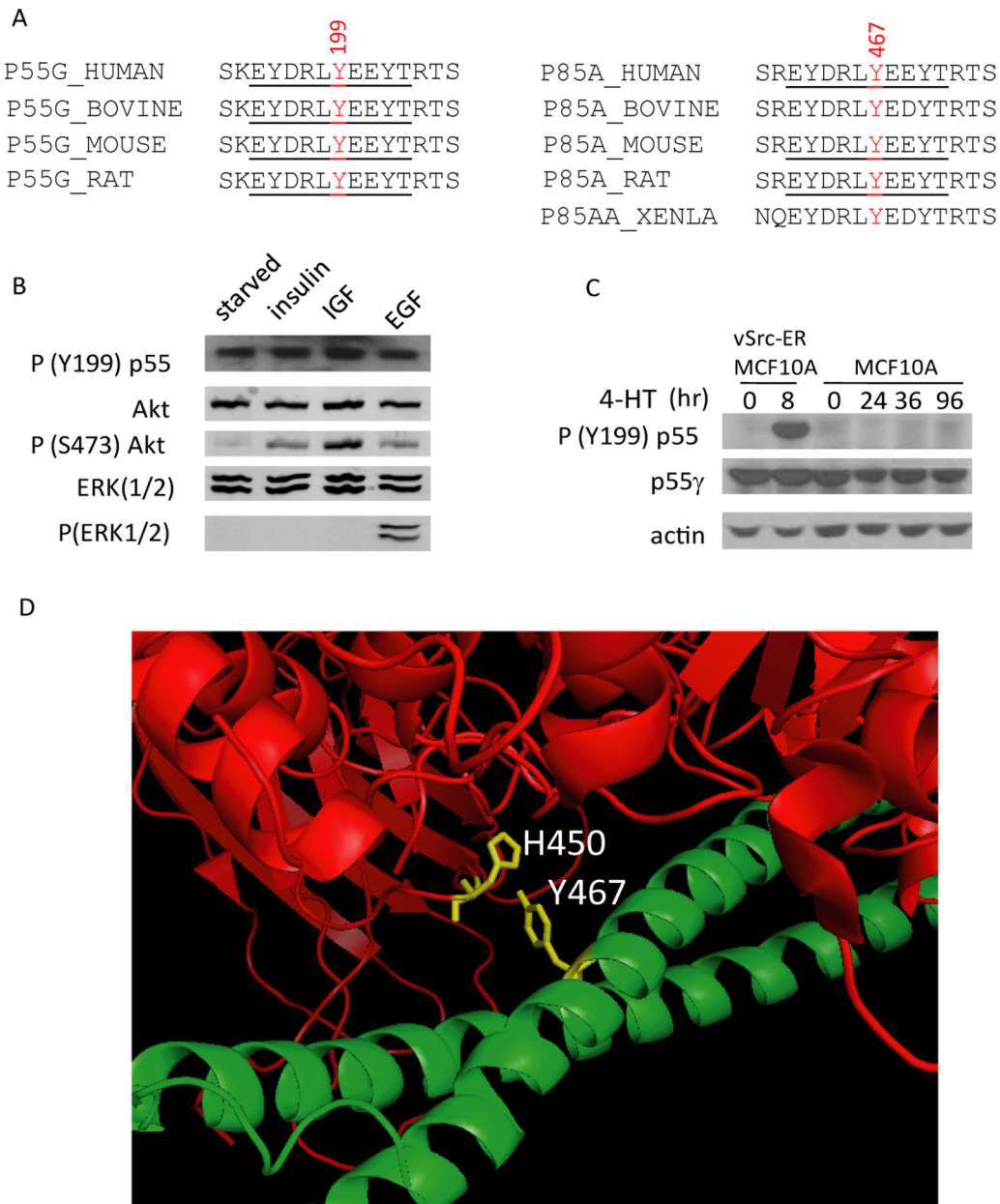


Fig. S6. Regulation of phosphorylation of p55 at Tyr-199. (A) Sequence alignment of the regulatory subunit of PI3K. Sequences corresponding to peptide H5 are underlined with the phosphorylated Tyr indicated in red. The sequences show high homology within different forms of the regulatory subunits among various species. (B) HEK293 cells were starved and stimulated with insulin, IGF, and EGF. Phospho-p55 (Tyr-199) levels were monitored using Western blotting analysis. (C) Phospho-p55 (Tyr-199) levels in MCF10A cells were not changed as a result of 4-HT treatment. MCF10A cells expressing ER:vSrc and MCF10A cells were treated with 1 μ M 4-HT for the indicated times. (D) Tyr-467/p85 α (correspondent of Tyr-199/p55 γ) is 2.7 Å away from His-450/p110 α in the crystal structure of PI-3 kinase, within the distance of potential hydrogen-bond formation (9). The structure was rendered with Pymol (The Pymol Molecular Graphics System). (Red) p110 α catalytic subunit and (green) p85 α regulatory subunit.

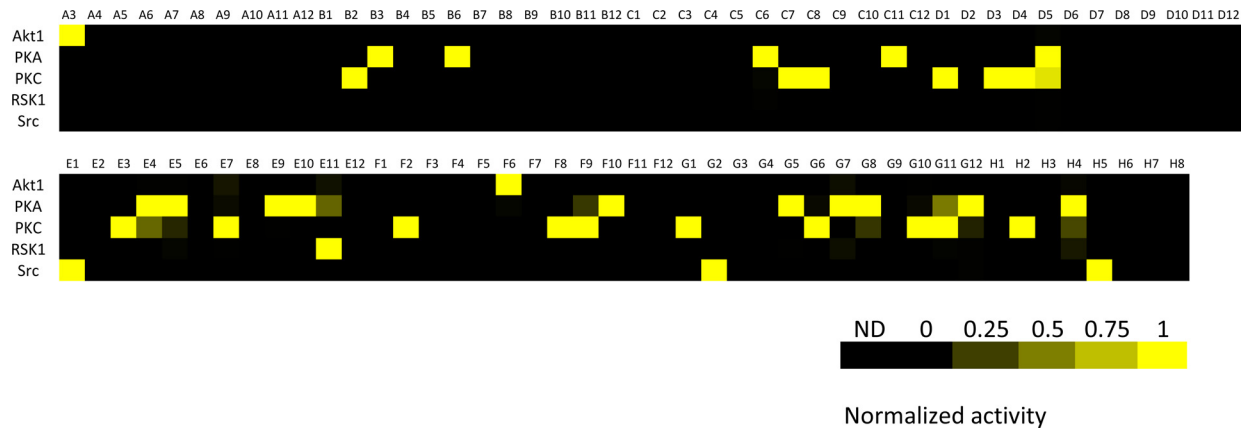


Fig. S7. Phosphorylation of the 90 KAYAK peptides in vitro using purified kinases. Two nanograms of kinase were used. Reaction conditions were the same as in Fig. S5. Activity of each peptide was normalized to the highest activity measured among the kinases examined (Akt1, PKA, PKC, RSK1, and Src). Highest activities of 2 fmol/ μ g/min were considered below detection threshold and shown as not detected (ND).

Table S1. Sequences of the peptides used in the KAYAK assay

ID	Substrate	Internal standard ^a	Site	Category ^b	Swiss-Prot ID	Protein name	Potential kinase ^c	MH+ (Sub)	MH+ (IS)
A3	RPRAATFPFR	RPRAATFPFR	t	S/T(B)	AKTIDE	aktide	Akt	1218.685	1304.672
A4	GPLAGSPVIApFR	GPLAGSPVIApFR	s	S/T(P)	SWISS;P19138;P20426;KC21_HUMAN	csnk2a1 protein	CDK	1281.731	1367.718
A5	LPGGSTPVSSpFR	LPGGSTPVSSpFR	t	S/T(P)	SWISS;P19138;P20426;KC21_HUMAN	csnk2a1 protein	CDK	1301.685	1387.671
A6	RPGPQSPGSPpFR	RPGPQSPGSPpFR	s	S/T(P)	SWISS;P14598;NCF1_HUMAN	neutrophil cytosol factor 1		1379.718	1465.704
A7	VGGAGYKQLpFR	VGGAGYKQLpFR	y	Y	SWISS;P42702;LIFR_HUMAN	leukemia inhibitory factor receptor precursor		1389.764	1475.750
A8	GGVNVYSGLPpFR	GGVNVYSGLPpFR	s	S/T(O)	SWISS;P40763;STAT3_HUMAN	signal transducer and activator of transcription 3		1391.707	1477.693
A9	EPLTPSGEAPPFR	EPLTPSGEAPPFR	t	S/T(P)	SWISS;P00533;P06268;EGFR_HUMAN	epidermal growth factor receptor precursor		1397.706	1483.692
A10	TPPSAYGSVKpFR	TPPSAYGSVKpFR	y	Y	SWISS;P07355;ANX2_HUMAN	annexin a2	Src	1406.743	1492.729
A11	APKKGSKKAVpFR	APKKGSKKAVpFR	s	S/T(B)	SWISS;P02278;H2B_HUMAN	histone h2b	PKA	1413.869	1499.855
A12	PSTNSPVLKpFR	PSTNSPVLKpFR	s	S/T(P)	SWISS;E5PL1;E5PL1_HUMAN	Separase	CDK	1429.780	1515.766
B1	GSAAPYLKTKpFR	GSAAPYLKTKpFR	y	Y	SWISS;P40763;STAT3_HUMAN	signal transducer and activator of transcription 3		1435.806	1521.792
B2	KKASFKAKKpFR	KKAsFKAKKpFR	s	S/T(B)	peptide KKASFKAKK	peptide KKASFKAKK	PKC	1435.890	1521.876
B3	AKTRSSRAGLPpFR	AKTRSSRAGLPpFR	s	S/T(B)	SWISS;P02261;H2A1_HUMAN	histone h2a	PKA	1446.829	1532.815
B4	IPINGSPRTpFR	IPINGSPRTpFR	s	S/T(P)	SWISS;P06400;RB_HUMAN	retinoblastoma-associated protein	CDK	1451.812	1537.798
B5	NQDPVPSLVpFR	NQDPVPSLVpFR	s	S/T(P)	SWISS;P08172;ACM2_HUMAN	muscarinic acetylcholine receptor m2	MAPK	1455.759	1541.745
B6	PKRKVsSAEGpFR	PKRKVsSAEGpFR	s	S/T(B)	SWISS;P05114;HMGN1_HUMAN	nonhistone chromosomal protein hmg-14	RSK	1458.818	1544.804
B7	VKRQSTPSApFR	VKRQSTPSApFR	s	S/T(B)	SWISS;Q93100;PKBB_HUMAN	phosphorylase b kinase regulatory subunit beta	CDK	1460.797	1546.783
B8	TPSLPPTPRpFR	TPSLPPTPRpFR	t	S/T(P)	SWISS;P10636;UPSP-TAU_HUMAN	microtubule-associated protein tau		1466.811	1552.798
B9	RTPKDSPGIPpFR	RTPKDSPGIPpFR	s	S/T(P)	SWISS;K56A1;RSK_HUMAN	ribosomal protein s6 kinase alpha-1	ERK	1467.807	1553.793
B10	TKRNSPPSPpFR	TKRNSPPSPpFR	s	S/T(P)	SWISS;P20020;ATCP_HUMAN	plasma membrane calcium-transporting atpase 1	PKA	1470.781	1556.768
B11	LKLSPPSSRpFR	LKLSPPSSRpFR	s	S/T(P)	SWISS;P20700;LAM1_HUMAN	lamin-b1	CDK	1471.838	1557.824
B12	VPPSPLSRHpFR	VPPSPLSRHpFR	s	S/T(O)	SWISS;P13807;GYS1_HUMAN	glycogen [starch] synthase	CKI	1476.807	1562.793
C1	PKGTGYIKTEpFR	PKGTGYIKTEpFR	y	Y	SWISS;P42224;STA1_HUMAN	signal transducer and activator of transcription 1-alpha/beta		1493.811	1579.797
C2	IPTGTPQRKpFR	IPTGTPQRKpFR	t	S/T(P)	SWISS;P52732;EG5_HUMAN	kinesin-like protein kif11 (kinesin-related motor protein eg5)	CDK	1498.849	1584.835
C3	GLPKSYLPQTpFR	GLPKSYLPQTpFR	y	Y	SWISS;P40189;IL6RB_HUMAN	interleukin-6 receptor beta chain precursor		1503.832	1589.818
C4	DSARVYENVGpFR	DSARVYENVGpFR	y	Y	SWISS;Q06124;PTNB_HUMAN	tyrosine-protein phosphatase non-receptor type 11		1509.744	1595.731
C5	LLKLASPELEpFR	LLKLASPELEpFR	s	S/T(P)	SWISS;P05412;AP1_HUMAN	transcription factor jun-d	CDK	1512.878	1598.865
C6	TKRSGSVYEPpFR	TKRSGSVYEPpFR	s	S/T(B)	SWISS;Q93100;PKBB_HUMAN	phosphorylase b kinase regulatory subunit beta	RSK	1523.796	1609.783
C7	LKKLGSKKPQpFR	LKKLGSKKPQpFR	s	S/T(B)	SWISS;Q9y5y9;SC10A_HUMAN	sodium channel protein type 10 subunit alpha	PKC	1526.953	1612.939
C8	GKAKVTGRWKpFR	GKAKVTGRWKpFR	t	S/T(B)	SWISS;P45379;TNNT2_HUMAN	troponin t	PKC	1530.902	1616.888
C9	KKSKISASRKpFR	KKSKISASRKpFR	s	S/T(B)	SWISS;P19429;TNNT3_HUMAN	troponin i	PKC	1532.938	1618.925
C10	AENAEYLVRVpFR	AENAEYLVRVpFR	y	Y	SWISS;P00533;EGFR_HUMAN	epidermal growth factor receptor precursor		1535.796	1621.783
C11	NKRKRGSVLpFR	NKRKRGSVLpFR	s	S/T(B)	SWISS;P16452;42_HUMAN	erythrocyte membrane protein band 4.2	RSK	1539.923	1625.909
C12	HLLAPSEEDHpFR	HLLAPSEEDHpFR	s	S/T(A)	SWISS;P08833;IBP1_HUMAN	insulin-like growth factor-binding protein 1 precursor		1547.760	1633.747
D1	RKTTASTRKVPpFR	RKTTASTRKVPpFR	s	S/T(B)	SWISS;P13569;CFTR_HUMAN	cystic fibrosis transmembrane conductance regulator	PKC	1547.913	1633.899
D2	APRRRSIRNPpFR	APRRRSIRNPpFR	s	S/T(B)	SWISS;P14598;NCF1_HUMAN	neutrophil cytosol factor 1		1553.877	1639.864
D3	KLGSF5FKKpFR	KLGSF5FKKpFR	s	S/T(O)	SWISS;P29966;MACS_HUMAN	myristoylated alanine-rich c-kinase substrate	PKC	1555.874	1641.861
D4	LKIQASFRGHpFR	LKIQASFRGHpFR	s	S/T(O)	SWISS;Q92686; NEUG_HUMAN	neurogranin	PKC	1556.881	1642.867
D5	IKRFGSKAHLpFR	IKRFGSKAHLpFR	s	S/T(B)	SWISS;P29475;NOS1_HUMAN	nitric-oxide synthase, brain	PKA	1556.917	1642.904
D6	SPQPEYVNPpFR	SPQPEYVNPpFR	y	Y	SWISS;P04626;ERB2_HUMAN	receptor tyrosine-protein kinase erbB-2		1558.765	1644.751
D7	NLLPLPEEPpFR	NLLPLPEEPpFR	s	S/T(P)	SWISS;P42224;STA1_HUMAN	signal transducer and activator of transcription 1-alpha/beta	MAPK	1558.826	1644.813
D8	LPVPEYINQSpFR	LPVPEYINQSpFR	y	Y	SWISS;P00533;P06268;EGFR_HUMAN	epidermal growth factor receptor precursor	EGFR	1559.822	1645.808
D9	VKSRWVSGSQpFR	VKSRWVSGSQpFR	s	S/T(B)	SWISS;P04049;KRAF_HUMAN	raf proto-oncogene serine/threonine-protein kinase	PKC	1562.819	1648.805
D10	FKNIVTPRTpFR	FKNIVTPRTpFR	t	S/T(P)	SWISS;P02686;MBP_HUMAN	myelin basic protein	CDK	1572.901	1658.887
D11	REVGDYGLHHPpFR	REVGDYGLHHPpFR	y	Y	SWISS;O60674;JAK2_HUMAN	tyrosine-protein kinase jak2		1573.787	1659.773
D12	RPQRATSNVFPpFR	RPQRATSNVFPpFR	t	S/T(B)	SWISS;P24844;MLRN_HUMAN	myosin regulatory light chain 2		1575.850	1661.837
E1	EPEGDYEEVLPpFR	EPEGDYEEVLPpFR	y	Y	SWISS;P14317;HS1_HUMAN	hematopoietic lineage cell-specific protein		1579.727	1665.714
E2	FDDPSYVNVQpFR	FDDPSYVNVQpFR	y	Y	SWISS;P29353;SHC1_HUMAN	shc-transforming protein 1		1583.749	1669.735
E3	KRKQISVRGLpFR	KRKQISVRGLpFR	s	S/T(B)	SWISS;P11217;PHS2_HUMAN	glycogen phosphorylase		1584.981	1670.967
E4	LLRGPWDPFPpFR	LLRGPWDPFPpFR	s	S/T(B)	SWISS;P04792;HS27_HUMAN	heat-shock protein beta-1	MAPKAPK2	1587.843	1673.829
E5	LKRSLSELEIPpFR	LKRSLSELEIPpFR	s	S/T(B)	SWISS;P11831;SRF_HUMAN	serum response factor		1587.922	1673.908
E6	PQEGLYNELQpFR	PQEGLYNELQpFR	y	Y	SWISS;P20963;CD3Z_HUMAN	t-cell surface glycoprotein cd3 zeta chain precursor	Lck/Fyn	1590.791	1676.777
E7	LLRLF5FKAPPpFR	LLRLF5FKAPPpFR	s	S/T(B)	SWISS;Q6PCC3_HUMAN	gamma-aminobutyric acid a receptor, gamma 2, isoform 1	PKC	1591.947	1677.934
E8	VQNPVYHNQpFR	VQNPVYHNQpFR	y	Y	SWISS;P00533;EGFR_HUMAN	epidermal growth factor receptor precursor		1595.808	1681.794
E9	EKRKNsILNPpFR	EKRKNsILNPpFR	s	S/T(B)	SWISS;P13569;CFTR_HUMAN	cystic fibrosis transmembrane conductance regulator	PKA	1598.913	1684.899

ID	Substrate	Internal standard ^a	Site	Category ^b	Swiss-Prot ID	Protein name	Potential kinase ^c	MH+ (Sub)	MH+ (IS)
E10	AKKRLSVERIPFR	AKKRLsVERIpFR	s	S/T(B)	SWISS;P11388;TOPA_HUMAN	dna topoisomerase 2-alpha	PKC	1599.981	1685.967
E11	RKRLISSVEDPFR	RKRLIsSVEDpFR	s	S/T(B)	SWISS;P49815;Tuberin_HUMAN	tuberin	RSK, Akt	1602.907	1688.894
E12	LFPRNYVTPVpFR	LFPRNyVTPVpFR	y	Y	SWISS;P62993;GRB2_HUMAN	growth factor receptor-bound protein 2		1605.890	1691.876
F1	VRRFNTANDDPFR	VRRFNtANDDpFR	t	S/T(B)	SWISS;P29474;NOS3_HUMAN	nitric-oxide synthase,		1607.804	1693.790
F2	KKGQESFKKQpFR	KKGQEsFKKQpFR	s	S/T(B)	SWISS;P06748;NPM_HUMAN	nucleophosmin	PKC	1607.902	1693.888
F3	FLQRYSDPTpFR	FLQRySDPTpFR	s	S/T(A)	SWISS;P00533;P06268;EGFR_HUMAN	epidermal growth factor receptor precursor		1613.807	1699.793
F4	RKLKDTDSEEPFR	RKLKDtDSEEpFR	t	S/T(A)	SWISS;P02593;CALM_HUMAN	calm1 protein	CKII	1620.834	1706.820
F5	RTYSLGSALRPpFR	RTYSLGsALRPpFR	s	S/T(O)	SWISS;P08670;VIME_HUMAN	vimentin		1620.897	1706.883
F6	RIRTQSFSLQpFR	RIRTQsFSLQpFR	s	S/T(B)	SWISS;P29474;NOS3_HUMAN	nitric-oxide synthase	RSK, Akt	1635.908	1721.894
F7	EPENDYEDVEpFR	EPENDyEDVEpFR	y	Y	SWISS;P14317;HS1_HUMAN	hematopoietic lineage cell-specific protein		1638.692	1724.678
F8	KPKDASQRRRpFR	KPKDAsQRRRpFR	s	S/T(B)	SWISS;P12931;SRC_HUMAN	proto-oncogene tyrosine-protein kinase src	PKC	1641.941	1727.927
F9	LLELSRRRIPFR	LLELSRRRipFR	s	S/T(O)	SWISS;P05198;IF2A_HUMAN	eukaryotic translation initiation factor 2 subunit 1		1642.986	1728.973
F10	KLRKVKQEEpFR	KLRKVsQEEpFR	s	S/T(B)	SWISS;P50552;VASP_HUMAN	vasodilator-stimulated phosphoprotein	PKA	1644.954	1730.941
F11	RKGHEYTNIKpFR	RKGHEyTNIKpFR	y	Y	SWISS;Q06124;PTNB_HUMAN	tyrosine-protein phosphatase non-receptor type 11		1645.892	1731.879
F12	VKRRDYLDLAPFR	VKRRDyLDLApFR	y	Y	SWISS;P07949;RET_HUMAN	proto-oncogene tyrosine-protein kinase receptor ret precursor		1648.928	1734.915
G1	VLLRPSRRVpFR	VLLRPsRRVpFR	s	S/T(O)	SWISS;P32745;SSR3_HUMAN	somatostatin receptor type 3		1652.034	1738.021
G2	ELQDDYEDLLPFR	ELQDDyEDLLpFR	y	Y	SWISS;P02730;B3AT_HUMAN	band 3 anion transport protein		1652.780	1738.767
G3	LDNPDYQDpFR	LDNPdYQDpFR	y	Y	SWISS;P00533;EGFR_HUMAN	epidermal growth factor receptor precursor		1654.750	1740.736
G4	TDKEYYTVKDPFR	TDKEyYTVKDPFR	y	Y	SWISS;P23458;JAK1_HUMAN	tyrosine-protein kinase jak1		1661.817	1747.803
G5	SKRRNSEFEIPFR	SKRRNsEFEIpFR	s	S/T(B)	SWISS;P17752;TPH1_HUMAN	tryptophan 5-hydroxylase 1	RSK	1665.882	1751.868
G6	KKKKFSFKKpFR	KKKKFsFKKpFR	s	S/T(B)	SWISS;P49006;MRP_HUMAN	marks-related protein	PKC	1666.031	1752.018
G7	RKRRSSYHVpFR	RKRRSsYHVpFR	s	S/T(B)	SWISS;Q99250;SCN2A_HUMAN	sodium channel protein type 2 subunit alpha	PKA	1675.925	1761.912
G8	FKRRSSKDTpFR	FKRRSsKDTpFR	s	S/T(B)	SWISS;Q05586;P35437;NMZ1_HUMAN	glutamate [nmda] receptor subunit zeta 1 precursor	PKC	1680.940	1766.927
G9	FKNDKSKTWQpFR	FKNDKsKTWQpFR	s	S/T(B)	SWISS;P06730;IF4E_HUMAN	eukaryotic translation initiation factor 4e	PKA	1681.881	1767.867
G10	KKKRFsFKKSpFR	KKKRFsFKKSpFR	s	S/T(B)	SWISS;P29966;MARCS_HUMAN	myristoylated alanine-rich c-kinase substrate	PKA	1684.017	1770.003
G11	KKRRSRKESpFR	KKRRRsRKESpFR	s	S/T(B)	SWISS;P02278;H2B_HUMAN	histone h2b	PKC	1703.030	1789.016
G12	IKKSWSRWTLpFR	IKKSWsRWTLpFR	s	S/T(B)	SWISS;Q03431;PTHr1_HUMAN	parathyroid hormone/parathyroid hormone-related peptide receptor		1704.970	1790.956
H1	HHIDYyKkTTPFR	HHIDYyKkTTPFR	y	Y	SWISS;P11362;FGFR1_HUMAN	basic fibroblast growth factor receptor 1 precursor		1705.881	1791.867
H2	WPWQVSLRTRpFR	WPWQVsLRTRpFR	s	S/T(O)	SWISS;P00747;PLMN_HUMAN	apolipoprotein		1728.944	1814.931
H3	HLEKKYVRRDPFR	HLEKKyVRRDpFR	y	Y	SWISS;P07333;CSF1R_HUMAN	macrophage colony-stimulating factor 1 receptor precursor	c-Fms	1743.977	1829.963
H4	RLRRLsTKYRpFR	RLRRLsTKYRpFR	s	S/T(B)	SWISS;Q05209;PTNC_HUMAN	tyrosine-protein phosphatase non-receptor type 12	PKA	1749.051	1835.037
H5	EYDRLyEETpFR	EYDRLyEETpFR	y	Y	SWISS;P27986;P85A_HUMAN	phosphatidylinositol 3-kinase regulatory subunit	Src	1780.818	1866.804
H6	HTGFLTEyVATRpFR	HTGFLTEyVATRpFR	y	Y	SWISS;P28482;MK01_HUMAN	mitogen-activated protein kinase 1	MEK	1794.929	1960.881
H7	TSFLLTPyVVTRpFR	TSFLLTPyVVTRpFR	y	Y	SWISS;P45983;MK08_HUMAN	mitogen-activated protein kinase 8		1797.006	1962.958
H8	IYKNDyYRKRpFR	IYKNDyYRKRpFR	y	Y	SWISS;P08922;ROS_HUMAN	proto-oncogene tyrosine-protein kinase ros precursor		1818.976	1904.963

^aLower case "p" indicates heavy Pro and lower cases s/t/y indicate phosphorylated Ser/Thr/Tyr residues, respectively.

^bThe 90 peptides were categorized into Ser/Thr-containing (S/T) or Tyr-containing (Y) peptides, with the S/T peptides further classified into different motif groups based on the following binary decision tree, P at + 1 (Pro-directed: P), 3 or more E/D at + 1 to + 4 (acidic: A), R/K at -3 (basic: B), D/E at + 1, + 2 or + 3 (A), 2 or more R/K at -5 to -1 (B), otherwise (O).

^cPotential kinases were attributed based on Swissprot and literatures. IS, internal standard; Sub, substrate.

Table S2. Examples of substrate peptide specificity for different cell states

ID	Sequence	Parent protein (Phosphorylation site)	I ^a	E	G1/S ^b	G2/M	Potential kinase
A3	RPRAATFPFR	Aktide ^c	↑↑	↑			Akt
A5	LPGGStPVSSPFR	casein kinase II subunit alpha (Thr344)				↑	CDK
A12	PSTNSsPVLKPFPR	separase (Ser1126)				↑	CDK
B4	IPINGsPRTPPFR	retinoblastoma-associated protein (Ser249)		↑		↑↑	CDK
B5	NQDPVsPSLVPFPR	muscarinic acetylcholine receptor m2 (Ser232)			↓↓	↓	MAPK
B6	PKRKVsSAEGPFR	nonhistone chromosomal protein hmg-14 (Ser6)		↑		↓	RSK
B11	LKLSPsPSSRPFR	lamin-b1 (Ser392)			↑	↑↑	CDK
C2	IPTGTtPQRKPFPR	kinesin-like protein kif11 (Thr927)				↑↑	CDK
C6	TKRSGsVVEPPFR	phosphorylase b kinase regulatory subunit b(Ser26)		↑		↓	RSK
C11	NKRRGsVPILPFPR	erythrocyte membrane protein band 4.2 (Ser247)		↑			RSK
D7	NLLPLsPEEFPFPR	STAT1 (Ser727)			↓↓	↓↓	MAPK
D10	FKNIVtPRTPPFR	myelin basic protein (Thr229)				↑↑	CDK
E10	AKKRLsVERIPFR	DNA topoisomerase 2-alpha (Ser29)		↑			RSK
E11	RKRLIsSVEDPFPR	tuberin (Ser1798)		↑		↓	Akt, RSK
F6	RIRTQsFSLQPFR	nitric-oxide synthase, endothelial (Ser1176)	↑	↑↑			Akt, RSK
G5	SKRRNsEFEIPFR	tryptophan 5-hydroxylase 1 (Ser58)		↑			RSK
H5	EYDRLyEEYTPFR	PI3-kinase p85/p55 subunit (Tyr467/Tyr199)				↑↑	Src

^aPeptides with changed phosphorylation in insulin- (I) and EGF- (E) stimulated conditions compared to starved HEK293 cells.

^bPeptides with changed phosphorylation during G1/S and G2/M phases compared to asynchronously growing HeLa cells. A change of more than + 2-fold or -2-fold is indicated by "↑↑" or "↓↓", respectively. A change of more than + 4- or -4-fold is indicated by "↑↑↑" or "↓↓↓", respectively.

^cBozinovski S, Cristiano BE, Marmy-Conus N, Pearson RB (2002) The synthetic peptide RPRAATF allows specific assay of Akt activity in cell lysates. *Anal Biochem* 305:32–39.